Technical Note

A phantom based laser marking workflow to visually assess geometric image distortion in magnetic resonance guided radiotherapy

Matthias Drobnitzky [*], Axel vom Endt, Andrew Dewdney

Siemens Healthcare GmbH, Magnetic Resonance, Erlangen, Germany

ABSTRACT

Magnetic resonance (MR)-only workflows require quality assurance due to potential dosimetric impacts of using geometry distorted MR images in radiotherapy planning. MR-visible silicone-based fiducials were arranged in regular 3D structures to cover extended imaging volumes. The scanner's patient marking workflow with a 2-axes movable laser bridge allowed to visually check geometric distortions of each MR reconstructed fiducial against its true position in 3D space. A measurement resolution and uncertainty of the order of 0.5 mm in sagittal and coronal, and 1 mm in transversal direction was found. The proposed workflow required 1 min of evaluation time per fiducial position, and a 9 min 3D MR volume acquisition.

1. Introduction

The need for control and quality assurance in the context of magnetic resonance (MR)-only workflows is obvious due to the potential dosimetric impact of using distorted MR images in radiotherapy planning [1,2]. Systematic assessments have been conducted in academic radiotherapy settings, however there is not yet a widely accepted standard for quality assurance [3–6]. MR distortion correction that addresses gradient nonlinearity is usually deeply nested into the image reconstruction of commercial MR scanners.

Gradient fields realized with finite size gradient coils cannot be perfectly linear towards the edges of the field of view, for physical reasons. A small amount of gradient nonlinearity is often deliberately used in the electromagnetic design of gradient coils, in order to keep its electrical inductance low, which in turn allows to reach high slew rates without violating peripheral nerve stimulation limits. During gradient coil manufacturing it is verified that the intended electromagnetic design is technically realized. This justifies to use distortion correction as part of image reconstruction [7,8].

A variety of commercially available distortion phantoms offer cloud-based evaluation of remaining distortions; unfortunately, their operation can usually not be verified. This study describes a simple and transparent workflow based on an easy-to-realize MR geometry phantom and a widely available patient marking workflow to check for uncorrected distortions in MR images.

2. Material and methods

2.1. Geometry phantom

A thin plastic skeleton was built from struts of defined lengths, based on the golden ratio (ZOMETOOL, Zoomworks Corp, USA). They were interconnected by 95 hollow spheres of 10 mm inner and 18 mm outer diameter, held in place at the edges of nine nested cubes of varying sizes up to 38 cm (Fig. 1a).

MR visible fiducials were realized by filling the spheres with room-temperature vulcanizing two-part condensation liquid silicone of low Shore hardness. To minimize air bubble entrapment for homogeneous MR depiction, all fiducials were vacuum degassed at 20 mbar over 10 min. The completed 3D phantom structure had a weight of 673 g.

2.2. MR scanner with laser bridge

The phantom was positioned on the patient table of a 3 T MR scanner (MAGNETOM Vida, Siemens Healthcare, Erlangen, Germany), with the spine radiofrequency (RF) coil removed, and imaged using the scanner's integrated body RF coil (Fig. 1b).

We used an external laser bridge with two movable laser axes (Fig. 1b) (DORADOnova MR3T with Direct Laser Steering option, and Aquarius calibration phantom, LAP GmbH, Lueneburg, Germany). Its spatial offset position was carefully calibrated relative to the MR gradient coil using the supplied alignment phantom: its internal MR-
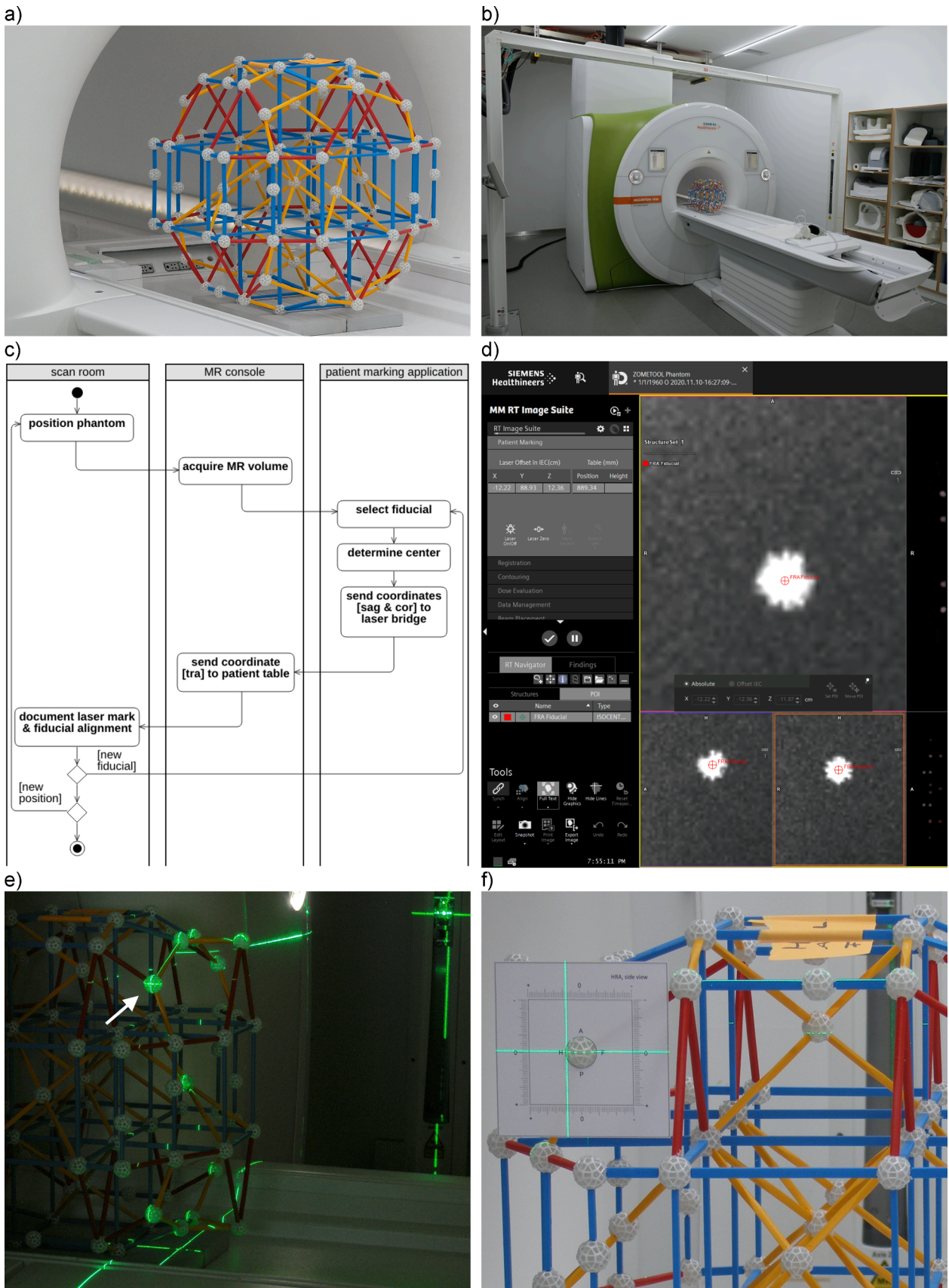

Fig. 1. a) ZOMETOOL realized geometry phantom consisting of 95 MR visible fiducials at defined positions, b) placed on the MR patient table, at the plane illuminated by the laser bridge. Exemplary visualization of the standard patient marking workflow, c) showing this study's evaluation workflow, d) determination of the center of the MR depicted fiducial, e) laser marking with fiducial coordinates sent to vertical and horizontal laser, and patient table, f) laser mark position measured with a paper scale.

visible crosshair structure corresponded to longitudinal and circumferential grooves on its outside which allowed to verify that all laser planes intersected the MR isocenter, and that the transversal laser planes run parallel to the transversal imaging plane of the MR scanner.

Laser bridge host and MR host were connected via network, which allowed the integrated patient marking application (syngo.via RT Image Suite, Siemens Healthcare, Erlangen, Germany) to send laser positioning commands to the bridge.

2.3. Laser marking workflow

This combination of medical devices allowed to execute the standard patient marking workflow as described by Ragan et al. [9] on the MR visible spherical fiducials: the selected fiducial was marked on orthogonal views of a volumetric MR acquisition, using coupled crosshair cursors, in all three directions. Using enlarged and interpolated fiducial visualization (Fig. 1d)) allowed to profit from subpixel resolution for the determination of its center position in the DICOM patient coordinate system, which under ideal conditions can be as low as 10% of pixel size for spherical fiducials [10]. Its reconstructed sagittal and coronal MR coordinates were sent to the horizontal and the vertical laser modules of the laser bridge, while its transversal coordinate was used to move the MR scanner's patient table, thereby bringing the respective fiducial into the crossing point of all movable lasers. The Direct Laser Steering option on the laser bridge in connection with syngo.via RT Image suite internally converted fiducial coordinates measured in the DICOM patient coordinate system to laser illumination coordinates defined according to IEC 61217.

Datasheet specifications of resolution and accuracy were given for vertical and horizontal laser marking, as well as the longitudinal patient table positioning: marking accuracy in this setup was technically limited to 0.5 mm, related to laser positioning and projection accuracy, and laser line width at the projection distance. The smallest distance for patient table movement was 1 mm, with an accuracy of 0.5 mm when moving from the same direction.

The position of the laser mark when projected on the related fiducial was examined at the MR scanner, with the phantom brought into the laser illumination plane (Fig. 1e). Printed scales for each examined fiducial were used to ease reading of the deviation of the laser mark relative to fiducial center position (Fig. 1f)).

The measurement resolution and uncertainty of the proposed workflow were examined in order to determine its capabilities to reproducibly measure geometric displacements of MR reconstructed fiducial positions against ground truth.

Measurement resolution was determined by controlled shifts of the patient table and the horizontal and vertical lasers, in manual operation mode.

Measurement uncertainty was experimentally determined within a single experimental setup, and additionally between experiments involving new phantom positionings, e.g. on the same or the following day (Fig. 1c)). A 9 min 3D gradient echo MR acquisition was used, for an isotropic resolution of 1.6 mm in each direction, with 288 slices covering a FOV of $500 \times 500 \times 460$ mm^3. The first test case alternatively used a head- and a feet-side fiducial for the marking workflow, placed at opposing sides of the phantom, at a relative distance of 244 mm, situated on a sphere of 425 mm. This procedure was then repeated for four times, inducing another eight table and eight laser module shifts, back and forth. This case was characteristic for determining the uncorrected distortions of a large number of widely spaced fiducials within one experiment. The second test case involved five completely new phantom setups, each measuring the same head- and feet-side fiducial for the marking workflow. This case was representative for checking the reproducibility of uncorrected distortions at FOV edges as part of regular scheduled quality assurance.

One experiment involving the head side fiducial was performed without distortion correction, and the reconstructed fiducial center then

projected on the phantom. This experiment was repeated with reverse readout gradient polarity [11], to allow to separate the influence of magnetic field inhomogeneities along the readout direction at the position of this fiducial from the geometric displacement due to gradient nonlinearity.

3. Results

As measurement resolution we found that shifts of the laser mark down to 0.5 mm could be reproducibly detected by visual comparison on printed scales, as well as all patient table shifts, that were limited to smallest possible increments of 1 mm.

Experimental findings for fiducial center selection uncertainty are shown in Fig. 2a and b: coordinates of fiducial centers were consistently close to each other, with an average absolute deviation from mean value of 0.12 mm, distributed over a range of 0.5 mm or smaller. Phantom repositioning resulted in an average absolute deviation from mean value of 0.18 mm in sagittal and coronal direction and 1.18 mm in transversal direction, distributed over ranges of 0.8 mm and 3.2 mm or smaller, respectively (Fig. 2c and d).

Measurement uncertainty can be seen as a shift of laser mark positions on fiducials, with all directions not larger than 0.21 mm as average absolute deviation from mean, distributed over a range of 1 mm or smaller (Fig. 2e and f).

An exemplary quality check of the geometric reconstruction accuracy of eight outer fiducials on the edges of the largest cube was done with the above described 9 min 3D gradient echo MR acquisition. Identification, selection, and marking a fiducial, sending laser and patient table coordinates and checking the accuracy at the scanner's bore in the laser illumination plane typically added 1 min of processing time per fiducial. Including documentation, this resulted in 20 min for this sample distortion check.

MR volumetric acquisition with distortion correction deliberately switched off allowed to study the effect of imperfect reconstruction of spatial position of fiducials: when using the dataset for the head side fiducial with the patient marking workflow, this resulted in projection of the laser cross on the fiducial at a position shifted by 9 mm towards head, consistent with numerical expectations from the electrical design of the gradient coil which had predicted a shift of 8.1 mm.

4. Discussion

The goal of this study was to derive a simple and transparent workflow based on an easy-to-realize MR geometry phantom and a widely available patient marking workflow to check for uncorrected distortions in MR images over large field of views. The measurement resolution of the described procedure was of the order of 0.5 mm in the sagittal and coronal, and 1 mm in the transversal plane, if a matching resolution for MR imaging was used. The measurement uncertainty was consistent with the technical limits for the position accuracy of laser modules and patient table. With optimized scanning protocols a dedicated distortion check including documentation could be completed in 20 min, thus allowing its integration into regular quality assurance procedures. The geometry phantom proved to be stable until now, over 6 month since initial construction, but had to be kept safely in a cardboard box when not in use. The silicone filling of the spherical fiducials remained mechanically stable and inert, without changing their MR signal strength over 9 month.

Other groups that quantified geometric distortions in MR imaging also used extended phantoms containing either spherical fiducials or regular grids. Based on volume MR acquisitions they derived distortion fields [3–6,12,13], or expanded the gradient nonlinearity in terms of spherical harmonic functions [14]. Unfortunately, MR images of spherical fiducials tended to undergo shape distortions when situated at the edges of the field of view, which made automated detection challenging. These phantoms were relatively lightweight, due to the small
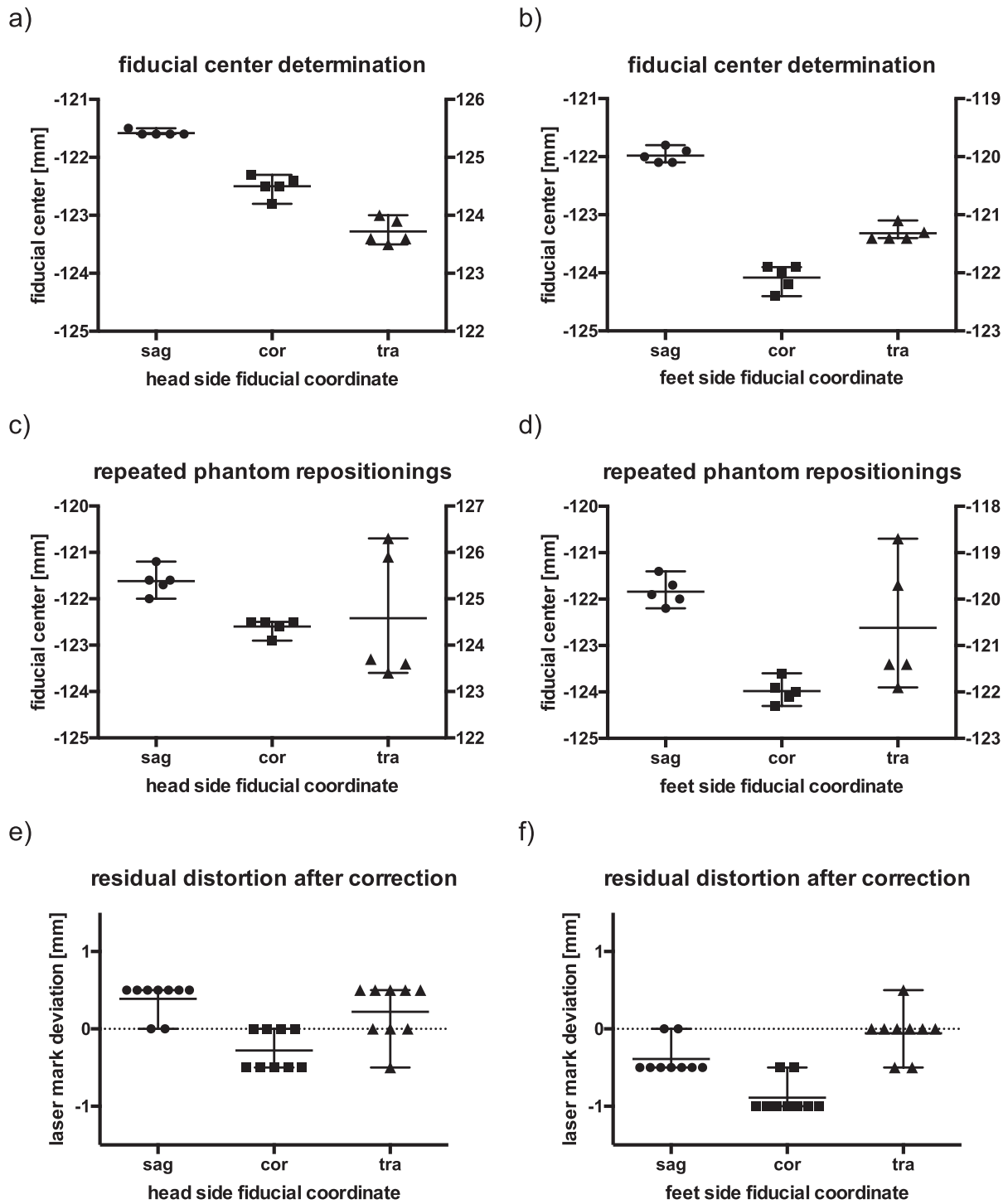
Fig. 2. Results for measurement uncertainty: distribution of sagittal, coronal and transversal coordinate of repeated fiducial center estimations from same phantom position, for a) head side fiducial, and b) feet side fiducial, and for repeated phantom repositionings, for c) head side fiducial, and d) feet side fiducial. Results for quality of distortion correction: laser mark deviation in mm, from fiducial center, along sagittal, coronal and transversal direction, for e) head side fiducial, and f) feet side fiducial.

amount of MR visible material concentrated in the fiducials. Grid-based phantoms use fiducials realized as grid intersections that are easier to follow due to the presence of dark lines. However these phantoms were heavy due to their liquid filling.

Measuring the magnetic field on a sphere that encompasses the to-be-probed gradient is another possibility that can be done using B0 field mapping devices, as described by Romeo et al. [15]. This procedures is

however sensitive to shim and eddy current compensation accuracy, and requires dedicated measuring tools to perform localized magnetic field strength measurements.

The type of phantom proposed in this study offers the advantage that it can be built to cover even large field of views with a total weight far below 1 kg. The proposed workflow does not require precise knowledge about the fiducial arrangement, ground truth from construction or from

another scan. However, it requires a carefully calibrated alignment of laser bridge and MR system. Our results indicate that it allows to visually determine remaining spatial distortions of MR imaging at arbitrary positions in very large field of views with accuracies of the order of 1 mm. The measurement resolution and uncertainty found in this study is similar to results reported by Wyatt et al. [4].

Main limitations of the present study is that fiducials are manually assessed one by one, in a sequential manner, which makes the procedure lengthy. The biggest advantage over fluid-filled or paintball-packed phantoms is its very low weight. Automated detection of fiducial centers would in principle be possible, with the risk of errors towards the edges of the field of view. In those difficult parts the manual determination of center fiducials was challenging, too. Manual note-taking about the positions of projected laser marks on fiducials is another potential source of errors.

Future work will be dedicated to building a phantom with larger and exactly spherical fiducials from MR-visible silicone, to profit from the achievable subpixel resolution for its center determination [10] in MR reconstructions. It is advisable to print 2D spherical coordinate on the fiducials to ease reading of laser mark positions with their rectilinear coordinates. Mechanical aids are needed to support reproducible positioning on the scanner's patient table.

In conclusion, an intuitive MR-only procedure was introduced that only employs systems present in many radiation therapy departments. The proposed workflow offers full transparency about the amount of geometric distortions, and is especially suited to raise awareness of radiation therapy professionals to MR-induced geometric distortions.

Declaration of Competing Interest

The authors declare the following financial interests/personal relationships which may be considered as potential competing interests: All three authors are employed by Siemens Healthcare GmbH, Erlangen, Germany, a manufacturer of MR scanners.

Acknowledgments

References

[1] Adjeiwaah M, Bylund M, Lundman JA, Söderström K, Zackrisson B, Jonsson JH, et al. Dosimetric impact of MRI distortions: a study on head and neck cancers. Int J Radiat Oncol Biol Phys 2019;103:994–1003. https://doi.org/10.1016/j.ijrobp.2018.11.037.

[2] Tanner SF, Finnigan DJ, Khoo VS, Mayles P, Dearnaley DP, Leach MO. Radiotherapy planning of the pelvis using distortion corrected MR images: the removal of system distortions. Phys Med Biol 2000;45:2117–32. https://doi.org/10.1088/0031-9155/45/8/305.

[3] Wang D, Doddrell DM, Cowin G. A novel phantom and method for comprehensive 3-dimensional measurement and correction of geometric distortion in magnetic resonance imaging. Magn Reson Imaging 2004;22:529–42. https://doi.org/10.1016/j.mri.2004.01.008.

[4] Wyatt J, Hedley S, Johnstone E, Speight R, Kelly C, Henry A, et al. Evaluating the repeatability and set-up sensitivity of a large field of view distortion phantom and software for magnetic resonance-only radiotherapy. Phys Imag Radiat Oncol 2018; 6:31–8. https://doi.org/10.1016/j.phro.2018.04.005.

[5] Adjeiwaah M, Garpebring A, Nyholm T. Sensitivity analysis of different quality assurance methods for magnetic resonance imaging in radiotherapy. Phys Imag Radiat Oncol 2020;13:21–7. https://doi.org/10.1016/j.phro.2020.03.001.

[6] Paulson ES, Erickson B, Schultz C, Li XA. Comprehensive MRI simulation methodology using a dedicated MRI scanner in radiation oncology for external beam radiation treatment planning. Med Phys 2015;42:28–39. https://doi.org/10.1118/1.4896096.

[7] Janke A, Zhao H, Cowin GJ, Galloway GJ, Doddrell DM. Use of spherical harmonic deconvolution methods to compensate for nonlinear gradient effects on MRI images. Magn Reson Med 2004;52:115–22. https://doi.org/10.1002/mrm.20122.

[8] Jovicich J, Czanner S, Greve D, Haley E, van der Kouwe A, Gollub R, et al. Reliability in multi-site structural MRI studies: effects of gradient non-linearity correction on phantom and human data. Neuroimage 2006;30:436–43. https://doi.org/10.1016/j.neuroimage.2005.09.046.

[9] Ragan DP, He T, Mesina CF, Ratanatharathorn V. CT-based simulation with laser patient marking. Med Phys 1993;20:379–80. https://doi.org/10.1118/1.597080.

[10] Efrat A, Gotsman C. Subpixel image registration using circular fiducials. Int J Comput Geom Appl 1994;04:403–22. https://doi.org/10.1142/S0218195994000223.

[11] Chang H, Fitzpatrick JM. A technique for accurate magnetic resonance imaging in the presence of field inhomogeneities. IEEE Trans Med Imaging 1992;11:319–29. https://doi.org/10.1109/42.158935.

[12] Price RG, Kadbi M, Kim J, Balter J, Chetty IJ, Glide-Hurst CK. Technical Note: characterization and correction of gradient nonlinearity induced distortion on a 1.0 T open bore MR-SIM. Med Phys 2015;42:5955–60. https://doi.org/10.1118/1.4930245.

[13] Tao S, Trzasko JD, Gunter JL, Weavers PT, Shu Y, Huston J, et al. Gradient nonlinearity calibration and correction for a compact, asymmetric magnetic resonance imaging gradient system. Phys Med Biol 2017;62:N18–31. https://doi.org/10.1088/1361-6560/aa524f.

[14] Tadic T, Jaffray DA, Stanescu T. Harmonic analysis for the characterization and correction of geometric distortion in MRI. Med Phys 2014;41:112303. https://doi.org/10.1118/1.4898582.

[15] Roméo F, Hoult DI. Magnet field profiling - analysis and correcting coil design. Magn Reson Med 1984;1:44–65. https://doi.org/10.1002/mrm.1910010107.